Circulation Research

ORIGINAL RESEARCH

Destabilization of Atherosclerotic Plaque by Bilirubin Deficiency

Weiyu Chen, Sergey Tumanov, Christopher P. Stanley, Stephanie M.Y. Kong, James Nadel, Niv Vigder, Darren L. Newington, Xiao Suo Wang, Louise L. Dunn, Roland Stocker

BACKGROUND: The rupture of atherosclerotic plaque contributes significantly to cardiovascular disease. Plasma concentrations of bilirubin—a byproduct of heme catabolism—inversely associate with risk of cardiovascular disease, although the link between bilirubin and atherosclerosis remains unclear.

METHODS: To assess the role of bilirubin in atherosclerotic plaque stability, we crossed *Bvra*$^{-/-}$ with *Apoe*$^{-/-}$ mice and used the tandem stenosis model of plaque instability. Human coronary arteries were obtained from heart transplant recipients. Analysis of bile pigments, heme metabolism, and proteomics were performed by liquid chromatography tandem mass spectrometry. MPO (myeloperoxidase) activity was determined by in vivo molecular magnetic resonance imaging, liquid chromatography tandem mass spectrometry analysis, and immunohistochemical determination of chlorotyrosine. Systemic oxidative stress was evaluated by plasma concentrations of lipid hydroperoxides and the redox status of circulating Prx2 (peroxiredoxin 2), whereas arterial function was assessed by wire myography. Atherosclerosis and arterial remodeling were quantified by morphometry and plaque stability by fibrous cap thickness, lipid accumulation, infiltration of inflammatory cells, and the presence of intraplaque hemorrhage.

RESULTS: Compared with *Bvra*$^{+/+}$*Apoe*$^{-/-}$ tandem stenosis littermates, *Bvra*$^{-/-}$*Apoe*$^{-/-}$ tandem stenosis mice were deficient in bilirubin, showed signs of increased systemic oxidative stress, endothelial dysfunction, as well as hyperlipidemia, and had a higher atherosclerotic plaque burden. Heme metabolism was increased in unstable compared with stable plaque of both *Bvra*$^{+/+}$*Apoe*$^{-/-}$ and *Bvra*$^{-/-}$*Apoe*$^{-/-}$ tandem stenosis mice and in human coronary plaques. In mice, *Bvra* deletion selectively destabilized unstable plaque, characterized by positive arterial remodeling and increased cap thinning, intraplaque hemorrhage, infiltration of neutrophils, and MPO activity. Proteomic analysis confirmed *Bvra* deletion enhanced extracellular matrix degradation, recruitment and activation of neutrophils, and associated oxidative stress in unstable plaque.

CONCLUSIONS: Bilirubin deficiency, resulting from global *Bvra* deletion, generates a proatherogenic phenotype and selectively enhances neutrophil-mediated inflammation and destabilization of unstable plaque, thereby providing a link between bilirubin and cardiovascular disease risk.

GRAPHIC ABSTRACT: A graphic abstract is available for this article.

Key Words: atherosclerosis ■ bilirubin ■ biliverdine ■ inflammation ■ oxidative stress ■ oxidoreductases ■ peroxidase

In This Issue, see p 791 | Meet the First Author, see p 792

Atherosclerosis is the major cause of cardiovascular disease (CVD), with rupture of vulnerable plaque and ensuing thrombosis thought to contribute significantly to CVD outcomes. Thin-cap fibroatheroma is a type of unstable plaque characterized by a thin fibrous cap, large lipid-rich necrotic core, high inflammatory cell content, and increased oxidative stress.[1] Prospective population-based cohort studies consistently show an inverse association between circulating total bilirubin concentrations and CVD risk.[2] Thus, individuals with moderate hyperbilirubinemia have a decreased risk of CVD. This is particularly the case for subjects with Gilbert syndrome—a

Correspondence to: Roland Stocker, PhD, Heart Research Institute, 7 Eliza St, Newtown, NSW 2042, Australia. Email roland.stocker@hri.org.au
Supplemental Material is available at https://www.ahajournals.org/doi/suppl/10.1161/CIRCRESAHA.122.322418.
For Sources of Funding and Disclosures, see page 826.
© 2023 American Heart Association, Inc.
Circulation Research is available at www.ahajournals.org/journal/res

Downloaded from http://ahajournals.org by on July 10, 2023

Novelty and Significance

What Is Known?

- The rupture of atherosclerotic plaque is the main cause of myocardial infarction, contributing significantly to the burden of cardiovascular disease.
- Plasma concentrations of bilirubin inversely associate with risk of cardiovascular disease, although the link between bilirubin and atherosclerosis remains unclear.
- Bilirubin has potential cardiovascular protective properties, including antioxidant and anti-inflammatory activities, as well as the ability to enhance endothelial function and suppress lipid accumulation.

What New Information Does This Article Contribute?

- Bilirubin deficiency induced by global *Bvra* gene knockout resulted in a proatherogenic phenotype, characterized by increased systemic oxidative stress, endothelial dysfunction, circulating lipids and atherosclerotic lesion size.
- Bilirubin deficiency also enhanced destabilization of unstable atherosclerotic plaque in a mouse model of plaque instability, characterized by increased positive arterial remodeling, thinning of the fibrous cap, inflammation, and myeloperoxidase activity, the latter of which has been reported recently to cause plaque destabilization.

To assess a potential link between bilirubin and atherosclerotic plaque rupture, we crossed bilirubin-deficient *Bvra*$^{-/-}$ mice with *apolipoprotein e* gene knockout (*Apoe*$^{-/-}$) mice, and subjected the resulting *Bvra*$^{-/-}$*Apoe*$^{-/-}$ animals to tandem stenosis (TS) surgery to induce formation of unstable plaques that share many features of thin-cap fibroatheroma in humans. Compared with littermate *Bvra*$^{+/+}$*Apoe*$^{-/-}$ TS mice, *Bvra*$^{-/-}$*Apoe*$^{-/-}$ TS mice had increased systemic oxidative stress, endothelial dysfunction, lipid accumulation and atherosclerotic lesion size. Moreover, *Bvra*$^{-/-}$*Apoe*$^{-/-}$ TS mice had increased plaque instability, intraplaque hemorrhage, and predilection to plaque rupture that was associated with increased positive arterial remodeling, heme degradation and inflammation. The latter included an increase in plaque activity of the proinflammatory and pro-oxidant enzyme myeloperoxidase, a process reported recently to cause plaque destabilization. The absence of bilirubin/BVRA (biliverdin reductase A) generates a hyperlipidemic proatherogenic phenotype that is characterized by hyperlipidemia, increased endothelial dysfunction, atherosclerosis, and plaque destabilization, providing a direct link between bilirubin and the risk of cardiovascular disease.

Nonstandard Abbreviations and Acronyms

BVR	biliverdin reductase
BVRA	biliverdin reductase A
CVD	cardiovascular disease
HMOX	heme oxygenase
IPH	intraplaque hemorrhage
MPO	myeloperoxidase
TS	tandem stenosis
UGT1A1	uridine diphosphate glucuronyl transferase

mild liver disorder where a mutation in UGT1A1 (uridine diphosphate glucuronyl transferase) attenuates hepatic conjugation of bilirubin for biliary excretion, resulting in a modest increase in circulating bilirubin.[3]

There are several mechanisms by which bilirubin may protect against CVD. Bilirubin has potent antioxidant activities[4,5] and acts synergistically with α-tocopherol to protect lipids from oxidation.[5] In addition, bilirubin has anti-inflammatory properties by attenuating monocyte chemotactic activity, adhesion of leukocytes to blood vessels, and the production of proinflammatory cytokines.[6–8] Moreover, bilirubin attenuates both activation of vascular endothelial cells and endothelial dysfunction, and it suppresses lipid accumulation and protects from adiposity.[9,10]

Despite well-established inverse associations, a causative link between bilirubin and CVD outcome has been impeded, in part, because of the low solubility of bilirubin in physiological buffers and its efficient biliary excretion via UGT1A1, making a supplementation approach difficult. Also, *Ugta1a1* gene-deficient mice develop severe hyperbilirubinemia after birth and do not survive past 1 week due to kernicterus.[11] As bilirubin is a product of heme degradation formed from biliverdin by biliverdin reductase, we generated a global *Bvra*$^{-/-}$ mouse as an experimental tool to assess in vivo functions of bilirubin: *Bvra*$^{-/-}$ mice have low concentrations of bilirubin and only slightly increased levels of biliverdin in plasma.[12] To assess the role of bilirubin in atherosclerosis related to CVD outcomes, we crossed *Bvra*$^{-/-}$ mice with *Apoe*$^{-/-}$ mice and subjected *Bvra*$^{-/-}$*Apoe*$^{-/-}$ animals to tandem stenosis (TS) as a model of plaque instability. In this model, the TS-induced low shear and high tensile stress gives rise to the formation of plaques with an unstable phenotype that share many features with culprit human lesions,[13] unlike the stable plaques seen in

Downloaded from http://ahajournals.org by on July 10, 2023

the standard *Apoe*$^{-/-}$ and *Ldlr*$^{-/-}$ mouse models. As the hemodynamic changes induced by the TS are limited to the right carotid artery,[13] unstable plaque in the TS model forms next to stable plaque in the brachiocephalic trunk, allowing for a direct comparison between unstable and stable plaques in the same animal.[13,14]

Here, we show that compared with littermate *Bvra*$^{+/+}$*Apoe*$^{-/-}$ TS animals, *Bvra*$^{-/-}$*Apoe*$^{-/-}$ TS mice have increased systemic oxidative stress, endothelial dysfunction, and plasma lipids. Moreover, unstable plaque in *Bvra*$^{-/-}$*Apoe*$^{-/-}$ TS mice is characterized by an increase in positive arterial remodeling, heme degradation, thinning of the fibrous cap, inflammation, and the activity of the pro-oxidant enzyme MPO (myeloperoxidase)—a process reported recently to cause plaque destabilization.[14] Proteomic profiling of unstable plaque confirmed enhanced extracellular matrix degradation, inflammation, and neutrophil degranulation in *Bvra*$^{-/-}$*Apoe*$^{-/-}$ compared with *Bvra*$^{+/+}$*Apoe*$^{-/-}$ TS mice. Our findings indicate a causative link between bilirubin deficiency due to *Bvra* (biliverdin reductase A) deletion and atherosclerotic plaque destabilization that may help explain existing epidemiological literature supporting a beneficial role for bilirubin against CVD.

METHODS

Data Availability

Raw data are available from the corresponding author upon reasonable request. The Major Resources Table is provided in the Supplemental Material.

The detailed experimental materials, methods, and data supporting the findings of this study are available within the article and its Supplemental Material.

Animals

The *Bvra*$^{-/-}$ mouse on C57BL/6J background has been described previously.[12] *Bvra*$^{-/-}$ mice were crossed with *Apoe*$^{-/-}$ mice on C57BL/6J background, and *Bvra*$^{+/+}$*Apoe*$^{-/-}$ and *Bvra*$^{-/-}$*Apoe*$^{-/-}$ littermate experimental animals were obtained from *Bvra*$^{+/-}$*Apoe*$^{-/-}$×*Bvra*$^{+/-}$*Apoe*$^{-/-}$ breeding pairs. All mice were housed in a temperature-controlled room on a 12-hour light/dark cycle and were allowed access to water and food ad libitum. All animal studies were approved by the Animal Welfare Committees of the Garvan Institute of Medical Research/St. Vincent's Hospital (protocol: 16-33), the University of New South Wales (protocol: 17-162B), and Sydney Local Health District (protocol: 2020-027). All procedures were performed according to the Guidelines for Animal Research outlined by the National Health and Medical Research Council of Australia and the Guide for the Care and Use of Laboratory Animals outlined by the National Institutes of Health.

TS Model of Plaque Instability

The TS model of plaque instability[13,14] was used throughout. Male mice at 6 weeks of age were fed a Western diet containing 22% fat and 0.15% cholesterol (SF00-219; Specialty Feeds, Western Australia) for 13 weeks. Six weeks after commencement of Western diet, TS surgery was performed to induce formation of unstable plaques proximal to the proximal suture, as described[13,14] (Figure S1). All TS surgeries were performed by the operator blinded to genotype. Briefly, *Bvra*$^{+/+}$*Apoe*$^{-/-}$ and *Bvra*$^{-/-}$*Apoe*$^{-/-}$ littermate mice were anesthetized with 4% isoflurane for induction followed by 2% isoflurane for maintenance. General anesthesia was confirmed by pedal reflex. An incision was made in the neck and the right common carotid artery dissected from circumferential connective tissues. Two ligatures were then placed, with the distal stenosis 1 mm from the carotid artery bifurcation and the proximal stenosis 3 mm from the distal ligature. Blood flow through the right common carotid artery was measured before and after placement of each ligature using a perivascular flow module (TS420; Transonic, NY) and a 0.7-mm perivascular flow probe (MA0.7PSB; Transonic). To ensure consistent TS constriction between each animal, the TS ligatures were tensioned to ensure blood flow through the carotid artery was reduced to 70% of baseline with placement of the first (distal) ligature and then reduced to 20% of baseline after placement of the second (proximal) ligature. To further ensure consistency of arterial constriction, a 150-µm needle (8-0, W1782, virgin silk blue; Ethicon) was placed on top of the exposed right common carotid artery to act as a guide as a 6-0 blue-braided polyester fiber suture was tied around both the artery and needle. The needle was then removed after TS ligature placement.

Statistical Analyses

Statistical analysis was performed using Graphpad Prism 9. Results are expressed as mean values with error bars representing SEM. Numeric data were first analyzed for normality using the Anderson-Darling, Shapiro-Wilk, and D'Agostino-Pearson tests. The statistical significance was then determined using the appropriate parametric (Student *t* test and repeated measures 2-way ANOVA) or nonparametric test (Mann-Whitney rank-sum test), as indicated in the figures. Precise *P* values with 2 significant digits are indicated in the figures.

RESULTS

Global *Bvra* Deletion Causes Bilirubin Deficiency and Increases Risk Factors for Atherosclerosis

Littermate *Bvra*$^{+/+}$*Apoe*$^{-/-}$ and *Bvra*$^{-/-}$*Apoe*$^{-/-}$ mice, fed Western diet for 13 weeks and subjected to TS surgery after 6 weeks of Western diet, had comparable body weight throughout the study duration (Figure 1A). As expected,[9,12] circulating concentrations of bilirubin were >150-fold lower and barely detectable in *Bvra*$^{-/-}$*Apoe*$^{-/-}$ (12±1 nM) compared with *Bvra*$^{+/+}$*Apoe*$^{-/-}$ TS mice (1902±308 nM; Figure 1B). The observed essential absence of bilirubin was accompanied by a comparatively modest (≈15-fold) increase in the plasma concentrations of biliverdin, from 7±1 to 117±10 nM in *Bvra*$^{+/+}$*Apoe*$^{-/-}$ versus *Bvra*$^{-/-}$*Apoe*$^{-/-}$ TS mice (Figure 1C).

Compared with *Bvra*$^{+/+}$*Apoe*$^{-/-}$, *Bvra*$^{-/-}$*Apoe*$^{-/-}$ TS mice were hyperlipidemic and showed signs of increased systemic oxidative stress, inflammation, and endothelial

Downloaded from http://ahajournals.org by on July 10, 2023

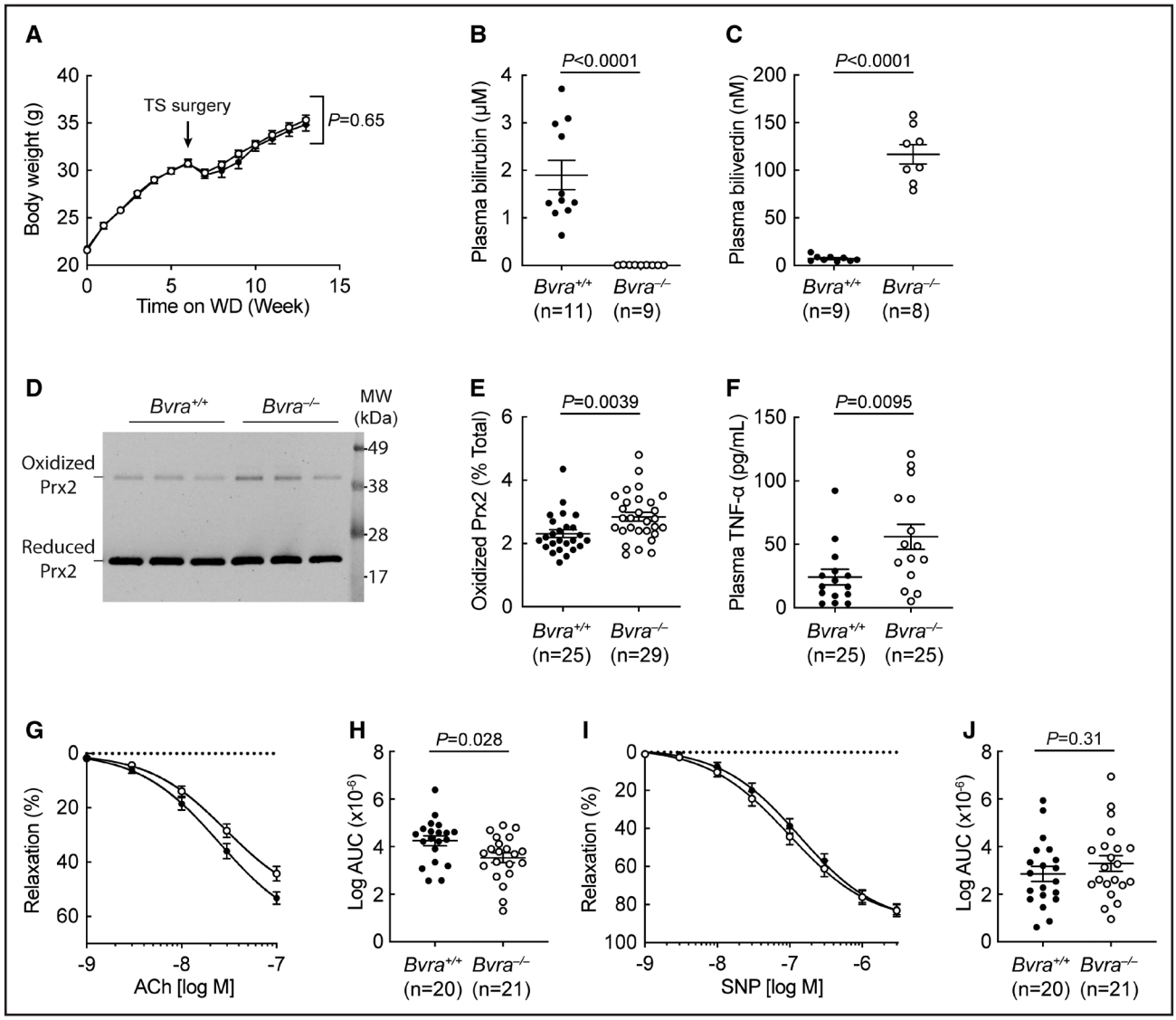

Figure 1. Systemic effects of global *Bvra* gene deletion in the tandem stenosis (TS) mouse model of plaque instability. **A**, Body weight of *Bvra*$^{+/+}$*Apoe*$^{-/-}$ (n=51) and *Bvra*$^{-/-}$*Apoe*$^{-/-}$ (n=49) mice fed a Western diet (WD) for 13 weeks, with TS surgery performed 6 weeks after commencement of WD. **B** and **C**, Plasma concentrations of bilirubin and biliverdin in *Bvra*$^{+/+}$*Apoe*$^{-/-}$ and *Bvra*$^{-/-}$*Apoe*$^{-/-}$ TS mice were determined by liquid chromatography tandem mass spectrometry. **D**, Representative redox Western blot showing Prx2 (peroxiredoxin 2) dimer (oxidized) and monomer (reduced) in blood cells of *Bvra*$^{+/+}$*Apoe*$^{-/-}$ and *Bvra*$^{-/-}$*Apoe*$^{-/-}$ TS mice. For unedited Western blot, see Figure S8. **E**, Densitometric analysis of Prx2 immunoblots obtained from whole blood cells of littermate *Bvra*$^{+/+}$*Apoe*$^{-/-}$ and *Bvra*$^{-/-}$*Apoe*$^{-/-}$ TS mice. **F**, Plasma concentration of TNF-α (tumor necrosis factor alpha) in *Bvra*$^{+/+}$*Apoe*$^{-/-}$ and *Bvra*$^{-/-}$*Apoe*$^{-/-}$ TS mice determined by ELISA. **G** through **J**, Relaxation of abdominal arteries isolated from *Bvra*$^{+/+}$*Apoe*$^{-/-}$ and *Bvra*$^{-/-}$*Apoe*$^{-/-}$ TS mice. Abdominal arterial rings were preconstricted with norepinephrine and subsequent relaxation responses to acetylcholine (ACh) and sodium nitroprusside (SNP) determined using wire myography. **H** and **J**, Area under the curve (AUC) for relaxation responses shown in **G** and **I**, respectively. Numerical results show individual data and mean±SEM, with data in **B** through **J** obtained from samples collected 7 weeks after TS surgery and analyzed by the Mann-Whitney *U* test in **B**, **C**, **E**, **F**, **H**, and **J**. Data in **A** were analyzed by repeated measures 2-way ANOVA. Filled and open circles correspond to *Bvra*$^{+/+}$*Apoe*$^{-/-}$ and *Bvra*$^{-/-}$*Apoe*$^{-/-}$ TS mice, respectively.

dysfunction. Hyperlipidemia was indicated by an increase in the plasma concentrations of cholesterol and cholesteryl linoleate (Table S1). As a result, plasma concentrations of total cholesterol and total cholesteryl esters were significantly increased in *Bvra*$^{-/-}$*Apoe*$^{-/-}$ compared with *Bvra*$^{+/+}$*Apoe*$^{-/-}$ TS mice (Table S1).

An increase in systemic oxidative stress in *Bvra*$^{-/-}$*Apoe*$^{-/-}$ TS mice was indicated by significantly higher plasma concentrations of cholesteryl ester hydroperoxides (Table S1) and a more oxidized redox state of Prx2 (peroxiredoxin 2) in whole blood of these mice compared with *Bvra*$^{+/+}$*Apoe*$^{-/-}$ TS animals (Figure 1D and 1E). Cholesteryl ester hydroperoxides are a major form of oxidized lipids in circulating lipoproteins,[15,16] while Prx2 is a highly abundant enzyme in red cells where it provides antioxidant protection against hydrogen peroxide and alkyl hydroperoxides by cycling between its reduced and disulfide oxidized forms, such that the redox state of Prx2 represents a sensitive in vivo maker of oxidative stress.[17] The increase in plasma

Downloaded from http://ahajournals.org by on July 10, 2023

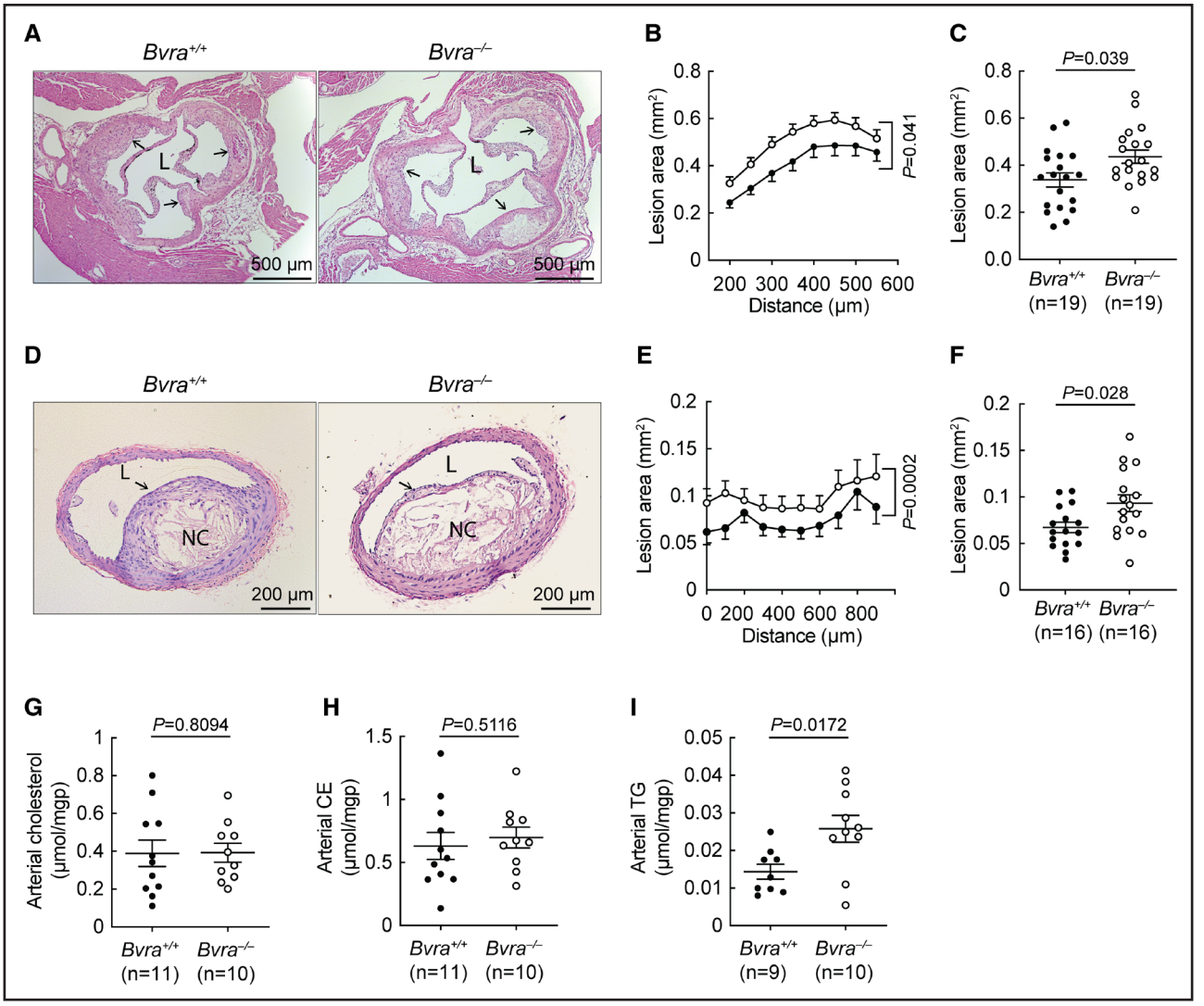

Figure 2. Bilirubin deficiency enhances atherogenesis in *Apoe*$^{-/-}$ tandem stenosis (TS) mice.
A–**F**, Morphometric analysis of atherosclerosis. **A**, Representative hematoxylin and eosin (H&E)-stained sections taken at the aortic root 300 μm distal from where all 3 aortic valve leaflets appear first. **B**, Lesion size in the ascending aorta of *Bvra*$^{+/+}$*Apoe*$^{-/-}$ and *Bvra*$^{-/-}$*Apoe*$^{-/-}$ TS mice was quantified from serial sections taken 200 to 550 μm distal to the aortic origin. **C**, Average lesion area in the aortic root at 200 and 350 μm distance from the aortic origin. **D**, Representative H&E-stained sections of the brachiocephalic artery 500 μm proximal to the bifurcation of the right subclavian and carotid artery. **E**, Lesion area in the brachiocephalic artery of *Bvra*$^{+/+}$*Apoe*$^{-/-}$ and *Bvra*$^{-/-}$*Apoe*$^{-/-}$ TS mice as assessed by serial cross-sections taken at specific distances from the bifurcation of the right subclavian and carotid artery. **F**, Average lesion area in the brachiocephalic artery at 0 to 900 μm distance from the bifurcation. **G**–**I**, Concentrations of cholesterol, cholesteryl esters (CE), and triacylglycerols (TG) in the brachiocephalic artery of *Bvra*$^{+/+}$*Apoe*$^{-/-}$ and *Bvra*$^{-/-}$*Apoe*$^{-/-}$ TS mice determined by high-performance liquid chromatography with ultraviolet detection (HPLC-UV), with results standardized to protein concentration. Data shown are obtained from samples collected 7 weeks after TS surgery and are presented as mean±SEM. Data in **B** and **E** were analyzed by repeated measures 2-way ANOVA, whereas data in **C** and **F**–**I** were analyzed by the Mann-Whitney *U* test. Arrows indicate the presence of atherosclerotic lesion. Filled and open circles correspond to *Bvra*$^{+/+}$*Apoe*$^{-/-}$ and *Bvra*$^{-/-}$*Apoe*$^{-/-}$ TS mice, respectively. L indicates lumen; and NC, necrotic core.

cholesteryl ester hydroperoxides in *Bvra*$^{-/-}$*Apoe*$^{-/-}$ TS mice was associated with a significant decrease in ubiquinol-9 (Table S1)—the major form of reduced coenzyme Q in mice[18] that forms the first line of antioxidant protection for lipoprotein-associated lipids.[16] Plasma concentrations of α-tocopherol were not significantly different between *Bvra*$^{+/+}$*Apoe*$^{-/-}$ and *Bvra*$^{-/-}$*Apoe*$^{-/-}$ TS mice (Table S1).

Systemic inflammation is prevalent in patients with atherosclerosis, and previous studies indicate that compared with standard *Apoe*$^{-/-}$ mice, *Apoe*$^{-/-}$ TS mice have increased systemic inflammation as assessed by circulating concentrations of TNF-α (tumor necrosis factor alpha).[19] *Bvra* deficiency further increased plasma concentration of TNF-α in *Apoe*$^{-/-}$ TS mice (Figure 1F), indicative of enhanced systemic inflammation. Plasma concentrations of interleukin-1β and interferon-γ were below or close to the detection limit (not shown), consistent with previous data.[19]

As markers of systemic inflammation and oxidative stress are associated with a fatty liver[20] and

Downloaded from http://ahajournals.org by on July 10, 2023

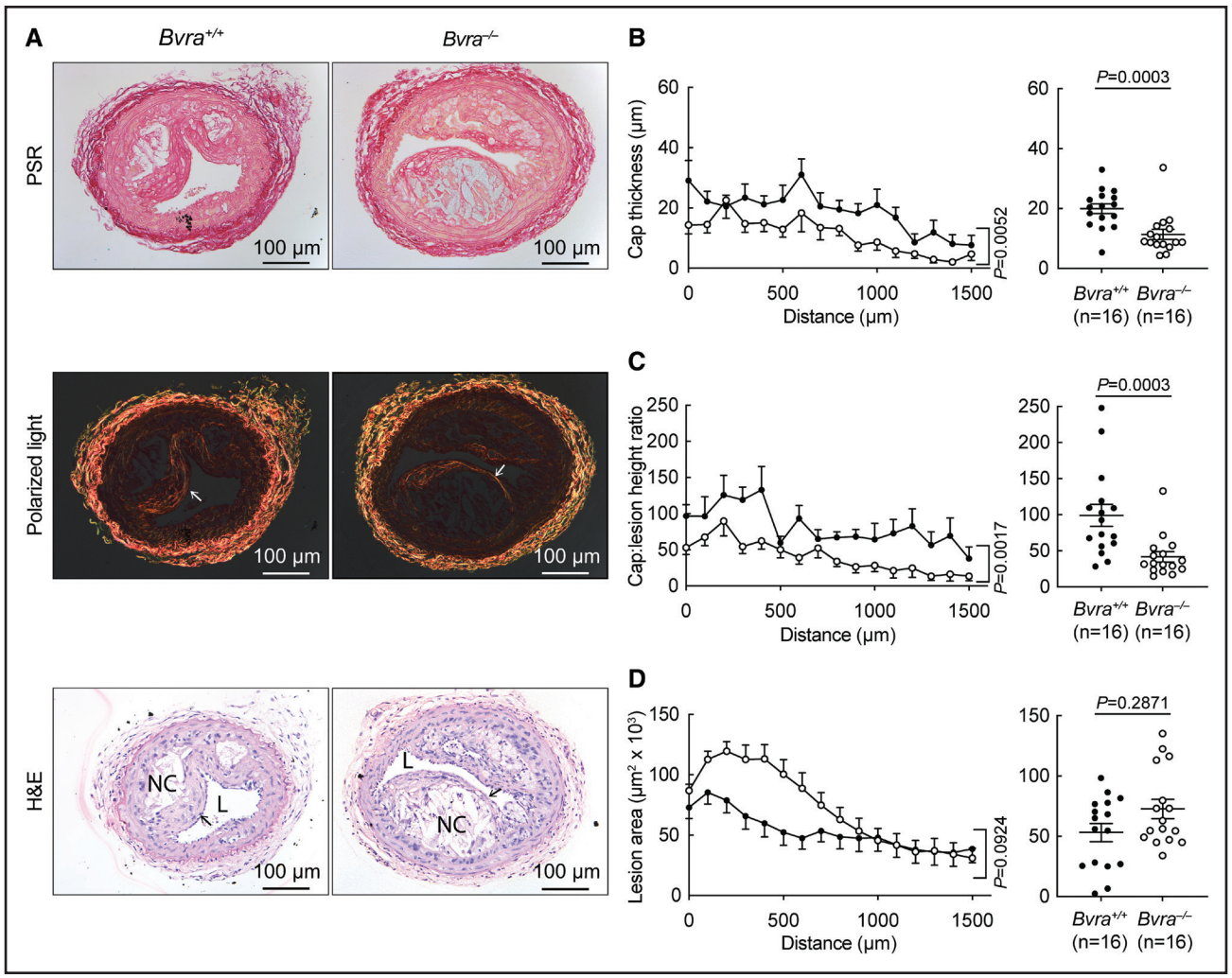

Figure 3. Bilirubin deficiency destabilizes atherosclerotic plaque as assessed by fibrous cap thickness.
A, Representative picrosirius red (PSR)–stained and hematoxylin and eosin (H&E)-stained sections of unstable plaque in *Bvra*$^{+/+}$*Apoe*$^{-/-}$ and *Bvra*$^{-/-}$*Apoe*$^{-/-}$ tandem stenosis (TS) mice taken 500 μm distal from the proximal suture and viewed under bright-field and polarized light. The arrow indicates the fibrous cap. Plaque stability was assessed by the cap thickness (**B**) and cap area-to-lesion height ratio (**C**). For **B** and **C**, data are shown throughout the arterial segment representing unstable plaque (**left**) and as averages (**right**). **D**, Atherosclerotic lesion size was determined in *Bvra*$^{+/+}$*Apoe*$^{-/-}$ and *Bvra*$^{-/-}$*Apoe*$^{-/-}$ TS mice throughout the entire arterial segment of the right carotid artery representing unstable plaque, with sections taken at 100-μm intervals from the proximal suture (**left**) and with average lesion areas (**right**). Results shown are obtained from samples collected 7 weeks after TS surgery and represent mean±SEM or individual results. Significance was evaluated using repeated measures 2-way ANOVA in **B**–**D** (**left**) and the Mann-Whitney *U* test in **B**–**D** (**right**). Filled and open circles correspond to *Bvra*$^{+/+}$*Apoe*$^{-/-}$ and *Bvra*$^{-/-}$*Apoe*$^{-/-}$ TS mice, respectively. L indicates lumen; and NC, necrotic core.

Bvra deficiency renders mice fed a high-fat diet susceptible to hepatic steatosis,[9] we examined *Bvra*$^{-/-}$*Apoe*$^{-/-}$ TS mice for signs of steatosis. The liver of *Bvra*$^{-/-}$*Apoe*$^{-/-}$ TS mice lacked bilirubin (Figure S2A through S2D), and the concentration of triacylglycerols—the most abundant class of hepatic lipids—was significantly increased compared with *Bvra*$^{+/+}$*Apoe*$^{-/-}$ TS littermates (Figure S2E through S2G). Moreover, plasma concentrations of asymmetric and symmetric dimethylguanidino valeric acid, that is, markers of nonalcoholic fatty liver disease,[21] were significantly increased in *Bvra*$^{-/-}$*Apoe*$^{-/-}$ compared with *Bvra*$^{+/+}$*Apoe*$^{-/-}$ TS mice (Figure S2H and S2I).

Endothelial dysfunction precedes atherosclerosis, and previous studies have shown that *Apoe*$^{-/-}$ TS mice have increased systemic endothelial dysfunction compared with standard *Apoe*$^{-/-}$ mice[19] and that bilirubin can attenuate endothelial dysfunction.[22] Therefore, we assessed endothelial function in the abdominal aorta of *Bvra*$^{-/-}$*Apoe*$^{-/-}$ and *Bvra*$^{+/+}$*Apoe*$^{-/-}$ TS mice using wire myography. *Bvra* deficiency significantly decreased endothelium-dependent relaxation induced by acetylcholine, whereas it had no material effect on endothelium-independent relaxation induced by sodium nitroprusside (Figure 1G through 1J), indicative of further enhanced systemic endothelial dysfunction in *Bvra*$^{-/-}$*Apoe*$^{-/-}$ TS mice.

Downloaded from http://ahajournals.org by on July 10, 2023

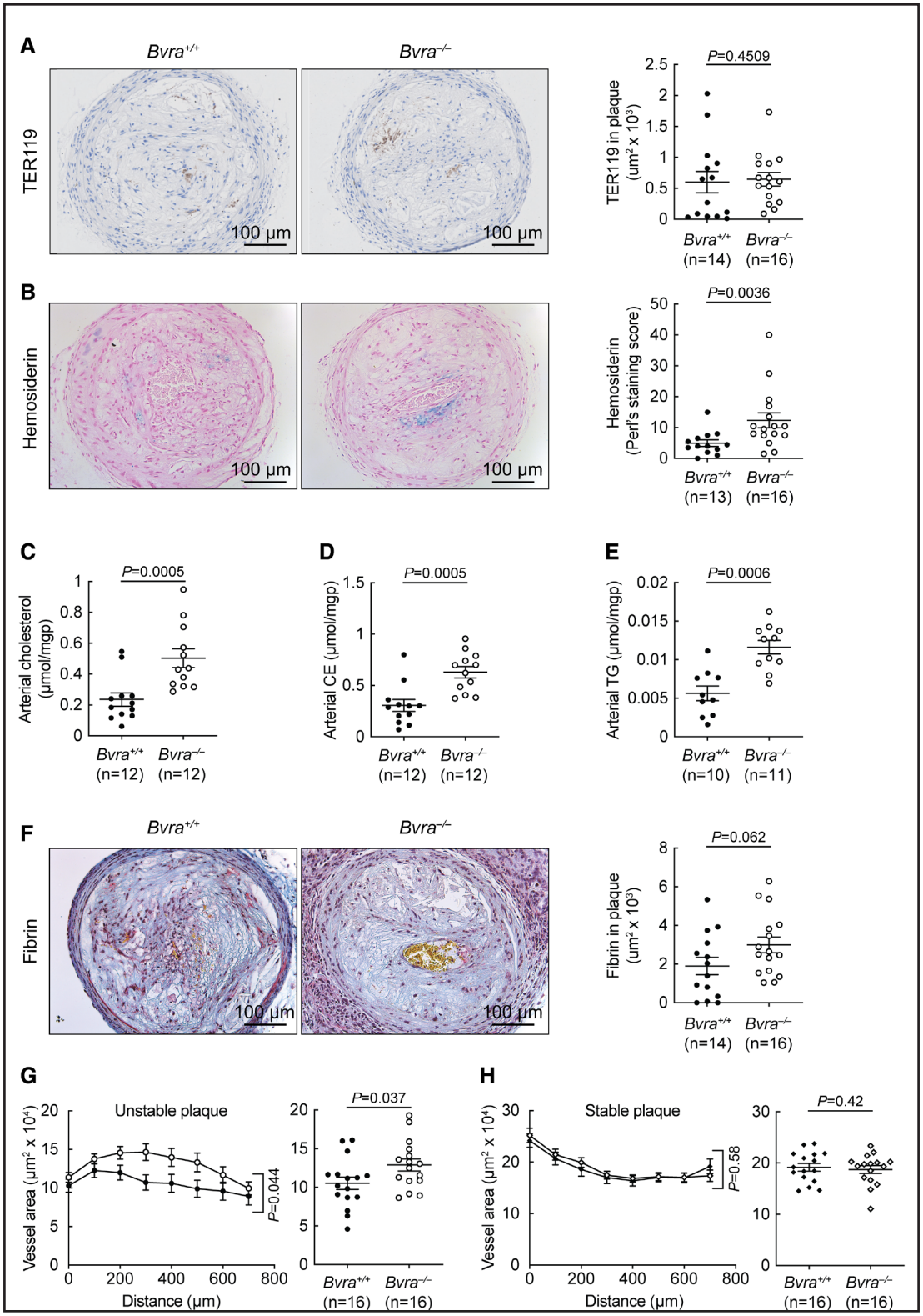

Figure 4. Bilirubin deficiency destabilizes atherosclerotic plaque as assessed by intraplaque hemorrhage, lipid content, and positive arterial remodeling.

A, Representative images of sections of unstable plaque in *Bvra*$^{+/+}$*Apoe*$^{-/-}$ and *Bvra*$^{-/-}$*Apoe*$^{-/-}$ tandem stenosis (TS) mice stained for TER119 (52 kD glycophorin A-associated protein, an erythroid-specific antigen also known as Ly-76), with TER119-positive region appearing in brown. Average area of TER119-positive area throughout the arterial segment representing unstable plaque (**right**). **B**, Representative images of sections of unstable plaque in *Bvra*$^{+/+}$*Apoe*$^{-/-}$ and *Bvra*$^{-/-}$*Apoe*$^{-/-}$ TS mice stained with Perls' Prussian blue, with hemosiderin-positive region appearing in blue. Average hemosiderin-positive area throughout the arterial segment representing unstable plaque is shown on the **right**. (*Continued*)

Downloaded from http://ahajournals.org by on July 10, 2023

Bilirubin Deficiency Due to Global *Bvra* Deletion Increases Atherogenesis and Destabilizes Atherosclerotic Plaque

The above findings show that the essential absence of bilirubin due to *Bvra* deletion results in hyperlipidemia and increased systemic oxidative stress, inflammation, and endothelial dysfunction, as well as hepatic steatosis. As these are all risk factors for atherosclerosis, we next examined the effect of global *Bvra* deletion on atherogenesis in *Apoe*$^{-/-}$ TS mice, assessed by morphometry as recommended by Daugherty et al.[23] *Bvra* deletion significantly increased the size of atherosclerotic lesions in both the aortic root and brachiocephalic artery, that is, sites where plaques with stable phenotype form (Figure 2A through 2F), and this was associated with a significant increase in the plaque content of triacylglycerols (Figure 2G through 2I). Increased atherogenesis observed in *Apoe*$^{-/-}$ TS mice deficient in endogenous bilirubin resulting from global *Bvra* deletion is consistent with a previous study reporting that administration of exogenous bilirubin decreased atherosclerosis at the aortic root of *Ldlr*$^{-/-}$ mice.[8]

In humans, serum bilirubin concentrations inversely associate with coronary plaque vulnerability as assessed by plaque fibrosis, lipid burden, and positive arterial remodeling,[24] that is, factors associated with increased susceptibility of plaques to rupture.[25] Therefore, we next determined plaque vulnerability in the arterial segment where unstable plaque develops in *Apoe*$^{-/-}$ TS mice, using cap thickness as primary readout[26] by quantifying collagen after picrosirius red staining and visualization under polarized light (Figure 3A). *Bvra* deletion significantly decreased plaque stability, whether determined as cap thickness (Figure 3B) or cap area-to-lesion height ratio (Figure 3C). Cap thinning by *Bvra* deletion was observed throughout the entire 1500 µm region (Figure 3B) and was examined to be independent of the overall burden of atherosclerosis (Figure 3D). Indeed, subanalyses of unstable plaque in arterial segments where lesion size was (0–1000 µm; Figure S3A) or was not significantly increased (1000–1500 µm; Figure S3B) confirmed cap thinning by *Bvra* deletion to be independent of its effect on atherogenesis (Figure S3C through S3F). Intriguingly, cap thinning by *Bvra* deletion was selective for unstable plaque, as it was not observed in stable plaque at the brachiocephalic trunk (Figure S3G and S3H).

We next assessed the contents of red cells, hemosiderin, lipids, and fibrin in unstable plaque as secondary readouts of plaque instability. *Bvra* deletion had no measurable effect on the expression of the erythrocyte marker TER119 (52 kD glycophorin A-associated protein) (Figure 4A), whereas it significantly increased Perls staining, which uses hemosiderin as a marker of long-term storage of iron derived from erythrocytes/hemoglobin and thus is indicative of intraplaque hemorrhage (IPH; Figure 4B).[27,28] Consistent with this observation, IPH was macroscopically visible in a greater proportion of *Bvra*$^{-/-}$*Apoe*$^{-/-}$ (60.4% or 32 of 53 animals) than *Bvra*$^{+/+}$*Apoe*$^{-/-}$ TS mice (46.3% or 25 of 54 animals). Moreover, *Bvra* deletion increased the content of lipids (triacylglycerols, cholesterol, and cholesteryl esters) in unstable plaque (Figure 4C through 4E), and there was a trend to increased fibrin deposition assessed by Martius Scarlet Blue staining (Figure 4F), suggestive of early progression of hemorrhage to fibrin-based clot formation.[28] Finally, *Bvra* deletion significantly increased positive remodeling in unstable (Figure 4G) but not stable plaque (Figure 4H). Together, these results indicate that *Bvra* deletion selectively enhances destabilization of unstable plaque in the *Apoe*$^{-/-}$ TS mouse model of plaque instability.

Increased Heme Metabolism Is a Feature Characteristic of Unstable Plaque

Heme metabolism is performed by the sequential action of HMOX (heme oxygenase) and BVR (biliverdin reductase), with biliverdin as intermittent product and bilirubin as end product, respectively (Figure 5A). Previous human and preclinical studies reported increased expression of HMOX1 protein to determine lesion progression to a vulnerable plaque,[29] although heme metabolism in stable versus unstable atherosclerotic plaque has not been determined previously. Therefore, we determined heme, biliverdin, and bilirubin in conjunction with the expression of HMOX1 and BVRA protein in stable and unstable plaque of *Bvra*$^{+/+}$*Apoe*$^{-/-}$ and *Bvra*$^{-/-}$*Apoe*$^{-/-}$ TS mice. Mean concentrations of heme were not statistically different in unstable versus stable plaque (Figure 5B),

Figure 4 Continued. C–**E**, Concentrations of cholesterol, cholesteryl esters (CE) and triacylglycerols (TG) in unstable plaque of *Bvra*$^{+/+}$*Apoe*$^{-/-}$ and *Bvra*$^{-/-}$*Apoe*$^{-/-}$ TS mice determined by high-performance liquid chromatography with ultraviolet detection, with results standardized to mg protein (mgp). **F**, Representative images of sections of unstable plaque in *Bvra*$^{+/+}$*Apoe*$^{-/-}$ and *Bvra*$^{-/-}$*Apoe*$^{-/-}$ TS mice stained with Martius Scarlet Blue, with fibrin-positive region appearing in red. Average area of fibrin-positive area throughout the arterial segment representing unstable plaque shown on the **right**. **G** and **H**, Arterial remodeling was assessed by morphometry of arteries representing stable and unstable plaque. **G**, Vessel area in the artery representing unstable plaque of *Bvra*$^{+/+}$*Apoe*$^{-/-}$ (n=16) and *Bvra*$^{-/-}$*Apoe*$^{-/-}$ TS mice (n=16) as assessed by serial cross-sections taken at 100-µm intervals from the proximal suture (**left**) and with average vessel area shown on the **right**. **H**, Vessel area in the artery representing stable plaque of *Bvra*$^{+/+}$*Apoe*$^{-/-}$ (n=16) and *Bvra*$^{-/-}$*Apoe*$^{-/-}$ TS mice (n=16) as assessed by serial cross-sections taken at 100-µm intervals from the bifurcation of the right subclavian and carotid artery (**left**) and with average vessel area shown on the **right**. Results shown are obtained from samples collected 7 weeks after TS surgery and represent the mean±SEM or individual results, with filled and open circles corresponding to *Bvra*$^{+/+}$*Apoe*$^{-/-}$ and *Bvra*$^{-/-}$*Apoe*$^{-/-}$ TS mice, respectively. Significance was evaluated using the Mann-Whitney *U* test for **A**–**F** and **G** (**right**) and **H** (**right**) and repeated measures 2-way ANOVA for **G** (**left**) and **H** (**left**).

Downloaded from http://ahajournals.org by on July 10, 2023

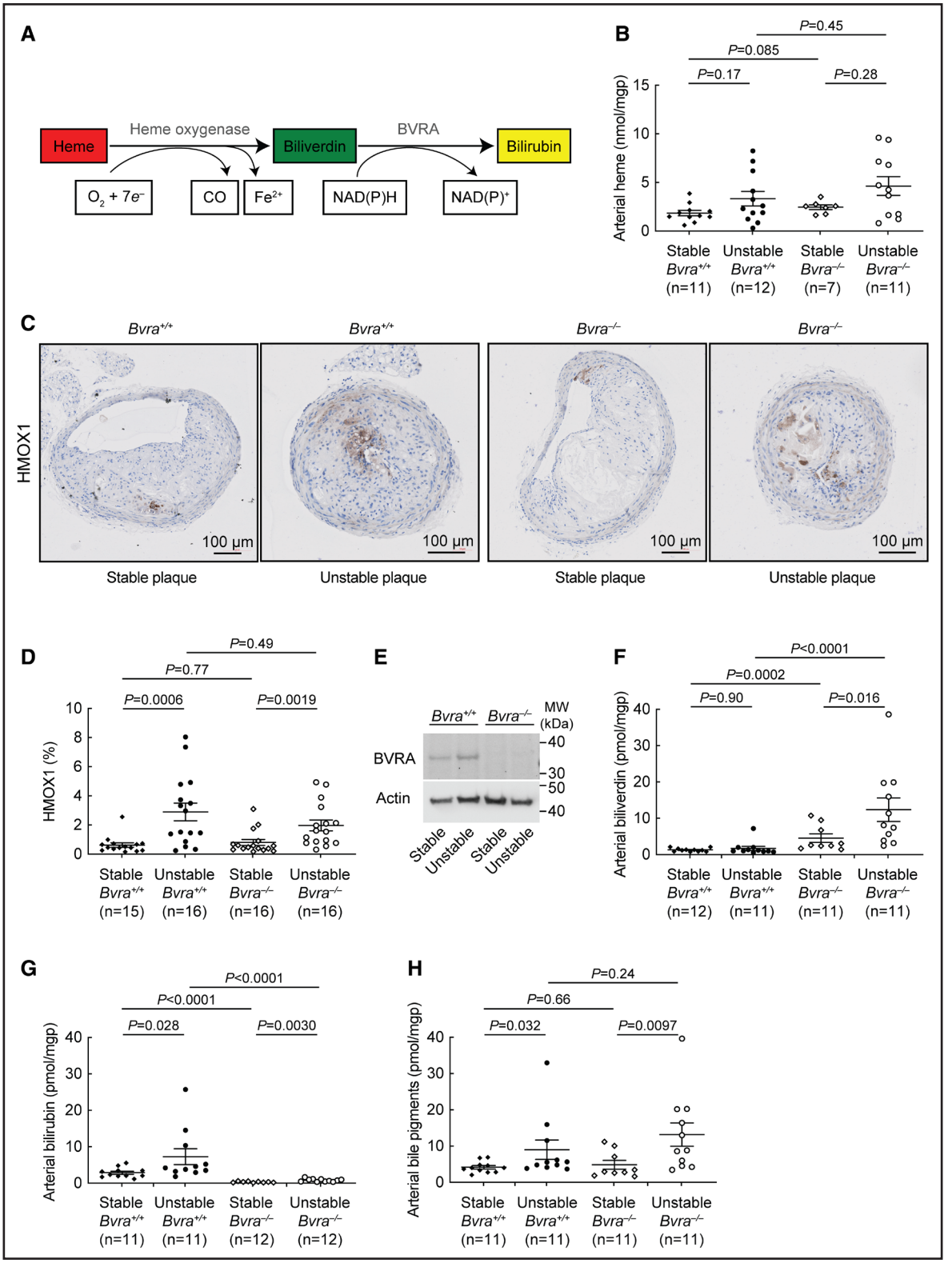

Figure 5. Increased heme metabolism in unstable compared with stable atherosclerotic lesions of *Bvra*$^{+/+}$*Apoe*$^{-/-}$ and *Bvra*$^{-/-}$*Apoe*$^{-/-}$ tandem stenosis (TS) mice.

A, Schematic of the heme metabolic pathway. **B** and **F**–**H**, Concentrations of heme, biliverdin, bilirubin, and total bile pigments in stable and unstable atherosclerotic plaque of *Bvra*$^{+/+}$*Apoe*$^{-/-}$ and *Bvra*$^{-/-}$*Apoe*$^{-/-}$ TS mice determined by liquid chromatography tandem mass spectrometry, with results normalized to protein content. **C**, Representative images of HMOX1 (heme oxygenase 1)-stained sections of stable and unstable plaque in *Bvra*$^{+/+}$*Apoe*$^{-/-}$ and *Bvra*$^{-/-}$*Apoe*$^{-/-}$ TS mice, with HMOX1^{+} region appearing in brown. **D**, Average area of HMOX1^{+} area throughout the arterial segment representing stable and unstable plaque. **E**, BVRA (biliverdin reductase A) expression in stable and unstable (*Continued*)

Downloaded from http://ahajournals.org by on July 10, 2023

whereas significantly more HMOX1 was expressed in unstable plaque (Figure 5C and 5D). The presence or absence of *Bvra* did not affect these parameters. BVRA was detected in both stable and unstable plaque of *Bvra*$^{+/+}$*Apoe*$^{-/-}$ but not *Bvra*$^{-/-}$*Apoe*$^{-/-}$ TS mice, as assessed by immunoblotting (Figure 5E; Figure S6). The small size of unstable and stable plaque meant that arterial segments from several animals had to be pooled for immunoblotting. Therefore, we next determined biliverdin and bilirubin by the more sensitive liquid chromatography tandem mass spectrometry analysis as a measure of heme metabolism. Arterial tissue concentrations of biliverdin were comparable (Figure 5F), whereas bilirubin and total bile pigments (biliverdin+bilirubin) were significantly increased in unstable compared with stable plaque (Figure 5G and 5H). *Bvra* deletion increased plaque concentrations of biliverdin to an extent that fully compensated for the observed decrease in arterial bilirubin in both stable and unstable plaque (Figure 5E through 5G). As a result, *Bvra* deletion had no material impact on the concentration of total bile pigment in stable and unstable plaque (Figure 5H). These results establish the presence of active heme metabolism in atherosclerotic lesions and show that heme metabolism is significantly increased in unstable compared with stable plaque independent of *Bvra* deletion. Together, these findings suggest that it is the absence of bilirubin rather than *Bvra* that associates with cap thinning of unstable plaque in *Bvra*$^{-/-}$*Apoe*$^{-/-}$ TS mice.

We next examined heme metabolism in stable and unstable plaque of human coronary arteries. Like *Apoe*$^{-/-}$ TS mice, HMOX1 protein was significantly more abundant in unstable than stable plaque (Figure 6A and 6B). Strikingly, increased HMOX1 expression was associated with the presence of IPH (Figure 6C) assessed histologically by Perls staining. Unlike in *Apoe*$^{-/-}$ TS mice, unstable human plaque had significantly higher concentrations of heme (Figure 6D), likely derived from red blood cells as reflected by the presence of IPH (Figure 6E). Biliverdin and bilirubin were similarly increased in unstable plaque and lesions with IPH (Figure 6F through 6I). As heme is a potent inducer of HMOX1 expression,[30] these findings indicate that in unstable human plaque, increased heme metabolism and a resultant increase in bilirubin is likely a compensatory response to the presence of IPH rather than causal to plaque instability. In addition to IPH, bilirubin concentrations also positively associated with the activity of the proinflammatory enzyme MPO (Figure 6J through 6L), consistent with plaque inflammation contributing to IPH and compensatory heme degradation.[31]

Bilirubin Deficiency Increases Inflammation in Unstable Plaque

As inflammation is a key contributor to atherosclerotic plaque vulnerability and rupture, we next determined arterial inflammatory cells in unstable plaque of *Bvra*$^{+/+}$*Apoe*$^{-/-}$ and *Bvra*$^{-/-}$*Apoe*$^{-/-}$ TS mice by IHC. As expected, unstable plaque showed pronounced staining for CD68 (monocytes) and LY6B.2 (neutrophils; Figure 7A). Such staining was generally stronger in unstable plaque of *Bvra*$^{-/-}$*Apoe*$^{-/-}$ TS mice and reached statistical significance for LY6B.2 (Figure 7A through 7C). As the proinflammatory enzyme MPO causes plaque destabilization in *Apoe*$^{-/-}$ TS mice,[14] we next determined the impact of bilirubin deficiency due to *Bvra* deletion on MPO protein and activity. Immunohistochemical analyses revealed that *Bvra* deletion significantly increased both MPO protein (Figure 7A and 7D) and chlorotyrosine (Figure 7A and 7E)—the latter representing a marker of MPO activity.[32] Noninvasive measurement of in vivo MPO activity by molecular magnetic resonance imaging using the MPO-specific sensor *bis*-5-hydroxytryptamide-DTPA-Gd (MPO-Gd) confirmed increased MPO activity in unstable plaque of *Bvra*$^{-/-}$*Apoe*$^{-/-}$ compared with *Bvra*$^{+/+}$*Apoe*$^{-/-}$ TS mice (Figure 7F and 7G). MPO activity assessed by chlorotyrosine protein adducts correlated positively with MPO protein and neutrophils (LY6B.2) rather than macrophages (CD68; Figure S5). Together, these findings show that bilirubin deficiency due to *Bvra* deletion increases plaque inflammation including MPO activity, which has been reported to cause plaque destabilization in *Apoe*$^{-/-}$ TS mice.[14]

Bvra Deletion Changes the Proteome of Unstable Plaque in *Apoe*$^{-/-}$ TS Mice

As a separate line of evidence for the potential mechanism of plaque instability induced by bilirubin deficiency, proteomic profiles of unstable plaque of *Bvra*$^{+/+}$*Apoe*$^{-/-}$ versus *Bvra*$^{-/-}$*Apoe*$^{-/-}$ TS mice were compared. We identified a total of 338 proteins, of which 31 proteins were significantly altered by >1.2-fold change ($\log_2$ transformed) between the 2 genotypes (Figure S7A). Protein-protein interaction networks functional enrichment analysis of the 31 proteins was performed using search tool for recurring instances of neighboring genes (STRING) (https://string-db.org; Figure S7B). COL1A2 (collagen type I alpha 2 chain), COL5A1 (collagen type V alpha 1 chain), COL6A1 (collagen type VI alpha 1 chain), COL6A3 (collagen type VI alpha 3 chain), DCN (decorin),

Figure 5 Continued. plaque as determined by immunoblotting. Arterial pools of stable and unstable plaque obtained from *Bvra*$^{+/+}$*Apoe*$^{-/-}$ and *Bvra*$^{-/-}$*Apoe*$^{-/-}$ TS mice (n=6 per genotype) were subjected to electrophoresis followed by transfer and immunoblotting using a polyclonal anti-BVRA antibody, with β-actin used as loading control. For uncropped Western blot, see Figure S6B. Results shown are from samples collected 7 weeks after TS surgery and represent individual results and mean±SEM, with open and filled diamonds corresponding to stable plaque and filled and open circles corresponding to unstable plaque of *Bvra*$^{+/+}$*Apoe*$^{-/-}$ and *Bvra*$^{-/-}$*Apoe*$^{-/-}$ TS mice, respectively. Significance between groups was evaluated using the Mann-Whitney *U* test.

Downloaded from http://ahajournals.org by on July 10, 2023

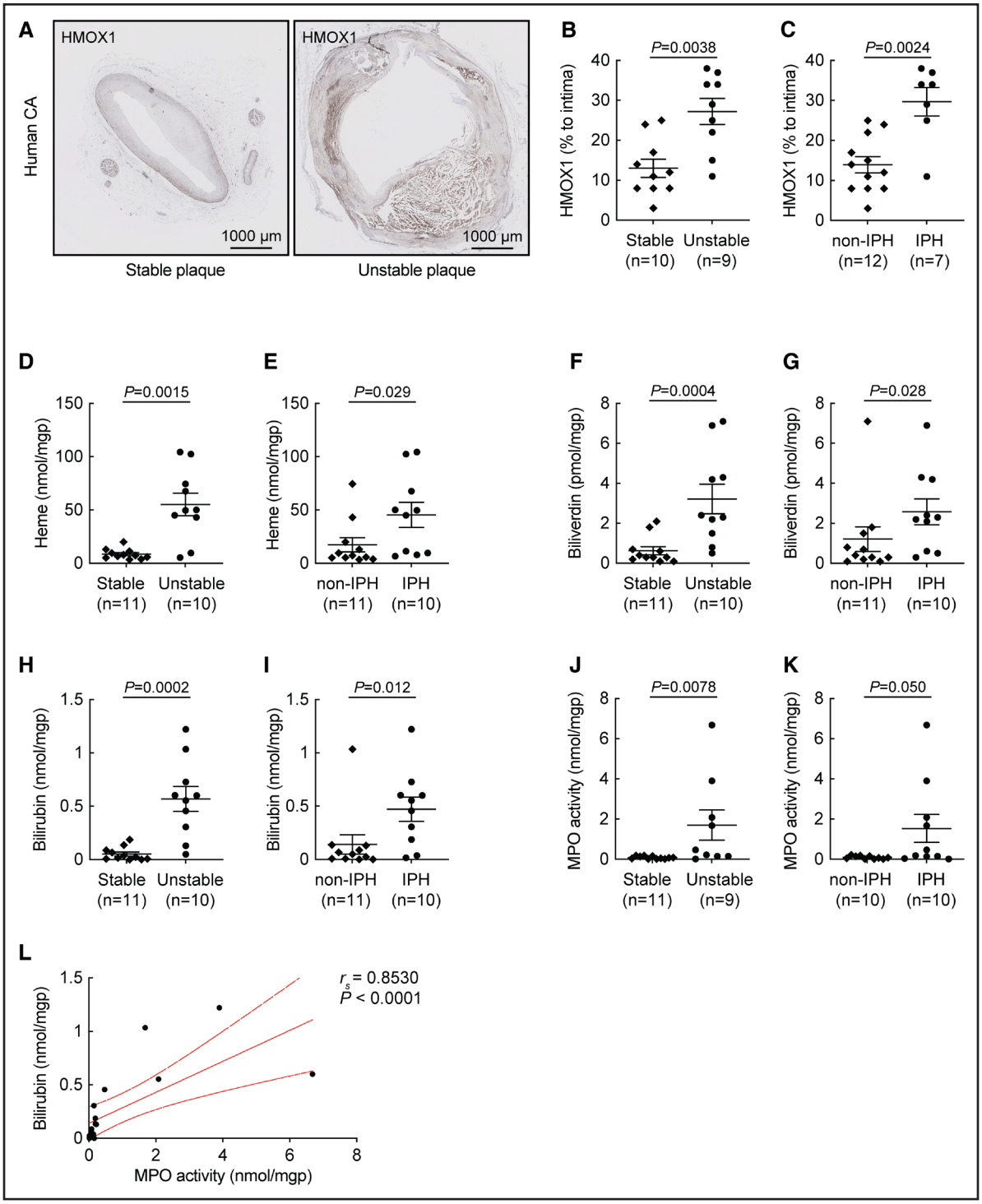

Figure 6. Increased heme metabolism in unstable atherosclerotic lesions of human coronary artery.
A, Representative images of HMOX1 (heme oxygenase 1)-stained sections of stable and unstable plaque in the human coronary artery, with HMOX1$^+$ region appearing in brown. **B** and **C**, HMOX1$^+$ area in tissue section of plaque with stable or unstable phenotype and plaque with or without intraplaque hemorrhage (IPH). **D** through **I**, Concentrations of heme, biliverdin, and bilirubin in human coronary arteries containing atherosclerotic plaque with stable or unstable phenotype and atherosclerotic plaque with or without IPH determined by liquid chromatography tandem mass spectrometry (LC-MS/MS), with results normalized to mg protein (mgp), respectively. **J** and **K**, MPO (myeloperoxidase) activity in human coronary artery plaque with stable or unstable phenotype, and plaque with or without IPH determined by LC-MS/MS, with results normalized to mgp. Significance was evaluated using the Mann-Whitney *U* test for **B**–**K**. **L**, Correlation between bilirubin concentration and MPO activity in human coronary plaque assessed by Spearman coefficient of rank correlation, r_s. Red solid and dotted lines represent the linear regression and 95% CI, respectively.

Downloaded from http://ahajournals.org by on July 10, 2023

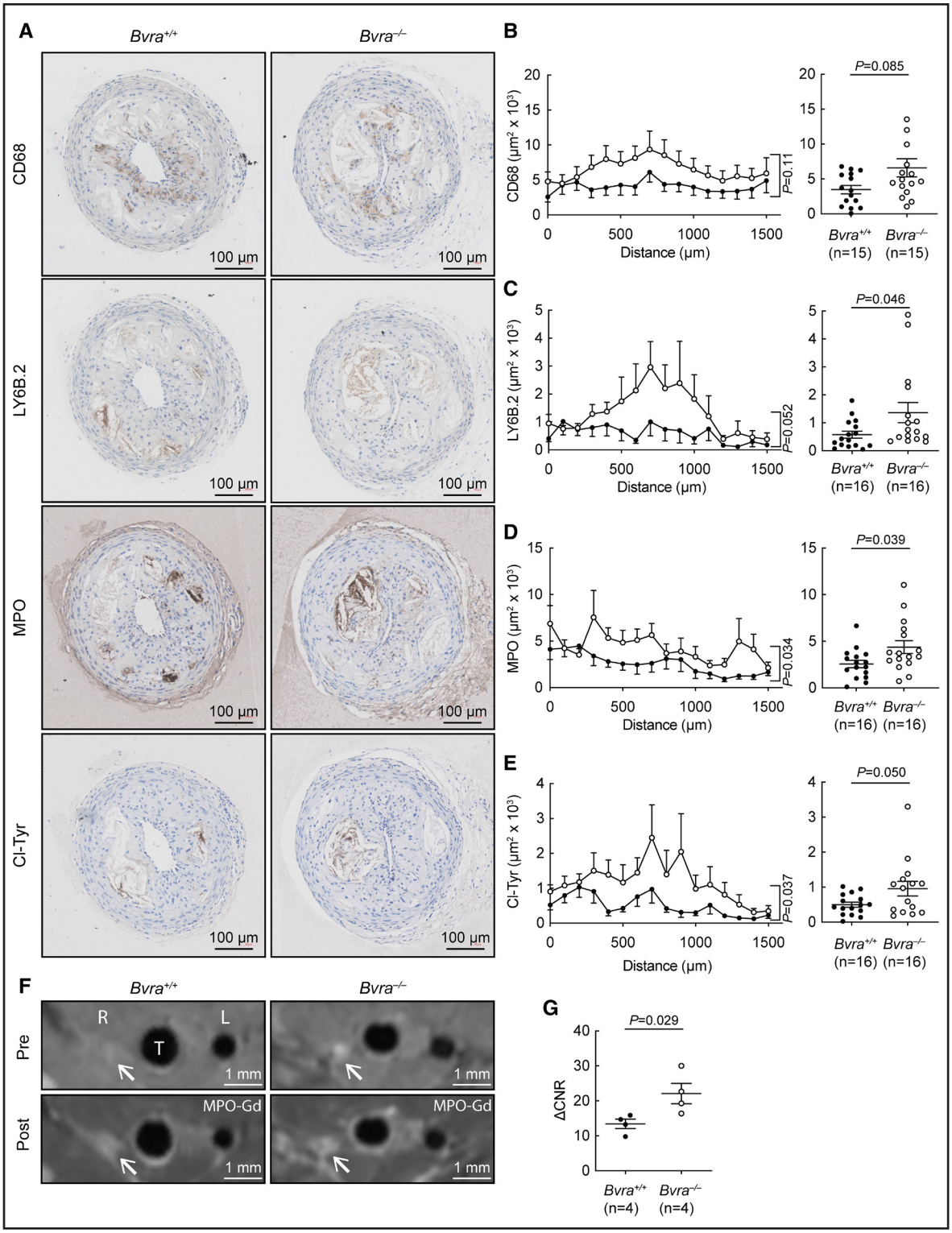

Figure 7. Bilirubin deficiency enhances inflammation in unstable atherosclerotic plaque.
A, Representative sections of unstable plaque stained for macrophages (CD68), neutrophils (LY6B.2), MPO (myeloperoxidase) protein, and chlorotyrosine (Cl-Tyr)—a measure of MPO activity. **B**–**E**, Arterial expression of CD68, LY6B.2, MPO, and Cl-Tyr was assessed throughout the arterial segment representing unstable plaque (**left**) and as averages (**right**). **F** and **G**, T1-TSE images of the right (R) and left (L) carotid arteries pre- and 60 minutes post-administration of MPO-Gd to *Bvra*$^{+/+}$*Apoe*$^{-/-}$ and *Bvra*$^{-/-}$*Apoe*$^{-/-}$ tandem stenosis (TS) mice with data expressed as the difference in contrast-to-noise ratio (ΔCNR) and calculated as $CNR_{60\ min}$—$CNR_{pre\text{-}contrast}$. Results shown are obtained from samples collected 7 weeks after TS surgery and represent mean±SEM or individual results, with filled and open circles corresponding to *Bvra*$^{+/+}$*Apoe*$^{-/-}$ and *Bvra*$^{-/-}$*Apoe*$^{-/-}$ TS mice, respectively. Arrow indicates the right carotid artery, T indicates trachea. Significance was evaluated using the repeated measures 2-way ANOVA in **B**–**E** (**left**) and the Mann-Whitney *U* test in **B**–**E** (**right**) and **G** (**right**).

Downloaded from http://ahajournals.org by on July 10, 2023

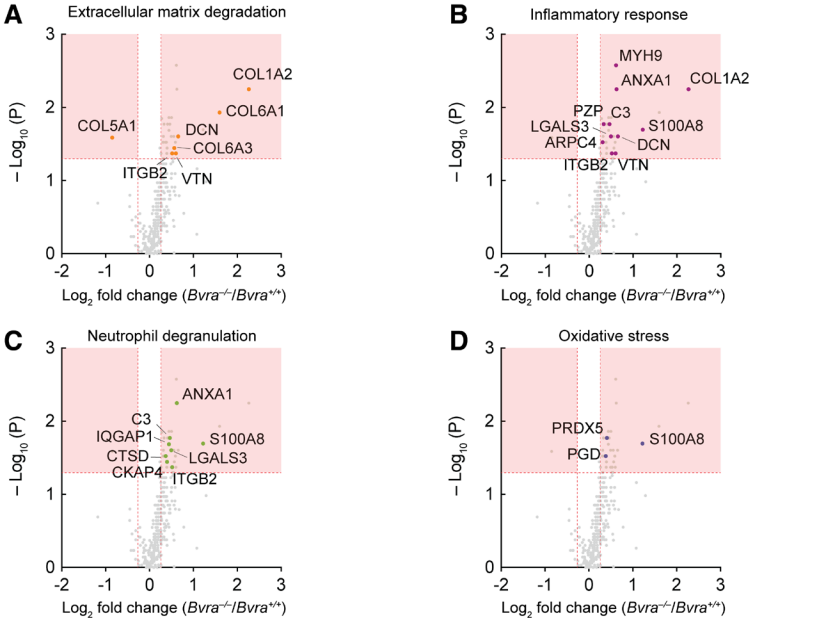

E

Description	Protein in network	Pathway
Extracellular matrix degradation	COL1A2, COL5A1, COL6A1, COL6A3, DCN, ITGB2, VTN	Collagen trimer (GO0005581), collagen degradation (MMU-1442490), extracellular matrix degradation (MMU-1474228), extracellular matrix organization (MMU-1474244)
Inflammatory response	ANXA1, ARPC4, C3, COL1A2, DCN, ITGB2, LGALS3, MYH9, PZP, VTN, S100A8	Inflammatory response pathway (WP458), increased inflammatory response (MP0001846)
Granulocyte chemotaxis and neutrophil degranulation	ANXA1, CTSD, CKAP4, C3, IQGAP1, ITGB2 LGALS3, S100A8	Granulocyte chemotaxis (GO0071621), neutrophil degranulation (MMU-6798695)
Oxidative stress	PGD, PRDX5, S100A8	Oxidative stress and redox pathway (WP4466)

Figure 8. Changes in protein abundance in unstable plaque resulting from *Bvra* deletion.
A–**D**, Proteomic analysis of unstable plaque of *Bvra*$^{+/+}$*Apoe*$^{-/-}$ (n=10) and *Bvra*$^{-/-}$*Apoe*$^{-/-}$ tandem stenosis (TS) mice (n=13). Volcano plots for 338 arterial proteins in unstable plaque were plotted with the *y* axis showing the $-\log_{10}$ (*P* value, unpaired) and the *x* axis showing the $\log_2$ fold change of protein abundance (*Bvra*$^{-/-}$*Apoe*$^{-/-}$/*Bvra*$^{+/+}$*Apoe*$^{-/-}$) calculated from the signal intensity values. The pink highlighted area denotes a fold change of >1.2 or <—1.2 and a *P* value <0.05. Dot points highlighted in orange (**A**), purple (**B**), green (**C**), and blue (**D**) are proteins related to extracellular matrix degradation, inflammatory response, neutrophil degranulation, and oxidative stress, respectively. **E**, Functional protein association networks assessed by search tool for recurring instances of neighboring genes (STRING) (protein-protein interaction networks functional enrichment analysis).

ITGB2 (integrin beta chain-2), and VTN (vitronectin) were among the significantly upregulated (downregulated for COL5A1) proteins. This indicated enhanced extracellular matrix degradation in unstable plaque of *Bvra*$^{-/-}$*Apoe*$^{-/-}$ compared with *Bvra*$^{+/+}$*Apoe*$^{-/-}$ TS mice, in support of the observed increased cap thinning and positive arterial remodeling in bilirubin deficiency (Figure 8A and 8E). In addition, we observed increases in ANXA1 (annexin A1), ARPC4 (actin related protein 2/3 complex subunit 4), C3 (complement component 3), COL1A2, ITGB2, LGALS3 (galectin 3), MYH9 (myosin-9), PZP (pregnancy zone protein), VTN, and S100A8 (calgranulin B), that is, proteins related to a proinflammatory response (Figure 8B and 8E). More specifically, proteins involved in neutrophil degranulation (ANXA1, CTSD [cathepsin D], CKAP4 [cytoskeleton-associated protein 4], C3, IQGAP1 [Ras GTPase-activating-like protein], ITGB2, LGALS3, and S100A8) were increased in unstable plaque of *Bvra*$^{-/-}$*Apoe*$^{-/-}$ TS mice (Figure 8C and 8E). Moreover, the expression of proteins related to oxidative stress, that is, PGD (phosphogluconate dehydrogenase), PRDX5 (peroxiredoxin 5) and S100A8, was increased (Figure 8D and 8E), potentially as a response to bilirubin deficiency. Combined with the observed increase in neutrophils and MPO activity in unstable plaque of *Bvra*$^{-/-}$*Apoe*$^{-/-}$ TS mice, the proteomic analysis confirmed that plaque destabilization by bilirubin deficiency due to *Bvra* deletion is caused by increased plaque inflammation associated with neutrophil infiltration and activation, including extracellular MPO activity.

DISCUSSION

The present study shows that systemic bilirubin deficiency resulting from global *Bvra* deletion generates a proatherogenic phenotype and selectively enhances the destabilization of unstable atherosclerotic plaque in the *Apoe*$^{-/-}$ TS mouse model of plaque instability. The observed enhancement of plaque destabilization was characterized by elevated plaque inflammation including increased activity of MPO—a proinflammatory and pro-oxidant enzyme recently reported to cause plaque

Downloaded from http://ahajournals.org by on July 10, 2023

destabilization.[14] The observed selectivity in destabilized plaque mirrored the selective increase in heme metabolism in unstable plaque and that was independent of the presence or absence of the *Bvra* gene. Together, our results indicate a causal role for bilirubin in atherosclerotic plaque stabilization that may help explain the inverse association between bilirubin and CVD outcomes.

Evidence for the increased proatherogenic phenotype in *Bvra*$^{-/-}$*Apoe*$^{-/-}$ TS mice is based on the observed hyperlipidemia and systemic oxidative stress, endothelial dysfunction, and proinflammatory state. Interestingly, hyperlipidemia in *Bvra*$^{-/-}$*Apoe*$^{-/-}$ TS mice was not limited to the circulation and atherosclerotic lesions but was also seen in the liver, consistent with the presence of a fatty liver in *Bvra*$^{-/-}$ mice fed a high-fat diet.[9] As epidemiological studies have established fatty liver as a risk factor for atherosclerosis and CVD,[33] the fatty liver observed in *Bvra*$^{-/-}$*Apoe*$^{-/-}$ TS mice may have contributed to the proatherogenic phenotype seen in these animals. Bilirubin has been reported to exert hypolipidemic effects via activation of peroxisome proliferator-activated receptor alpha[10] and the suppression of lipid oxidation.[9] Moreover, bilirubin decreases the hepatic expression of 3-hydroxy-3-methylglutaryl-CoA reductase in *Apoe*$^{-/-}$ mice, in association with inhibition of cholesterol synthesis and a decrease in circulating cholesterol, fatty liver formation, and atherogenesis.[34] However, that study examined the effect of bilirubin on atherosclerosis lesion size, whereas the present article focuses on the effect of the bile pigment on atherosclerotic plaque composition and stability.

A key advantage of the *Apoe*$^{-/-}$ TS mouse model over the conventional mouse models of atherosclerosis is that disease burden can be studied in the same animal in conjunction with plaque instability. The latter is important because it is well established that plaque composition and biological activity determine plaque instability and the associated increased potential for plaque rupture and ensuing thrombosis and thereby significantly contributing to CVD outcomes.[35] The present study provides several separate lines of evidence for bilirubin deficiency resulting from *Bvra* deletion to increase plaque destabilization, including fibrous cap thinning and an increase in plaque lipid deposition, inflammatory cell content, MPO activity and IPH, as well as positive remodeling. Strikingly, increased plaque destabilization was observed only in unstable plaque of *Apoe*$^{-/-}$ TS mice, in parallel with heme metabolism and associated formation of bilirubin being selectively elevated in unstable plaque of these animals. This selective increase in heme metabolism in unstable plaque was confirmed in human coronary lesions (Figure 6), consistent with a previous study using carotid endarterectomy specimens[29] and epidemiological studies reporting lower circulating concentrations of bilirubin in patients with acute coronary syndrome than patients with stable angina pectoris or control subjects.[24] Increased heme metabolism in unstable plaque of *Apoe*$^{-/-}$ TS mice and human coronaries correlated positively with TER119 (Figure S5) and Perls staining (Figure 6), respectively, suggesting it to be a consequence of IPH and resultant breakdown of red blood cell–derived heme, that is, processes largely absent in stable plaque.

Strikingly, increased heme metabolism in unstable compared with stable plaque of *Apoe*$^{-/-}$ TS mice was observed independent of the presence or absence of the *Bvra* gene, as assessed by the expression of HMOX1 and the concentration of total bile pigments (Figure 5), suggesting that plaque destabilization relates to the activities of bilirubin rather than BVRA. Induction of HMOX1 is complex.[30] While heme is an effective inducer of HMOX expression, several other factors need to be considered in the context of atherosclerotic plaques, in both *Bvra*$^{-/-}$*Apoe*$^{-/-}$ TS mice and human carotid arteries. These include both physical (eg, high and low blood flow, vascular injury) and chemical stress (eg, oxidative stress, oxidized lipids, and inflammation), such that the absence of a difference in plaque heme content between *Bvra*$^{+/+}$*Apoe*$^{-/-}$ TS and *Bvra*$^{-/-}$*Apoe*$^{-/-}$ TS mice per se does not rule out a difference in HMOX1 expression. Additional studies are required to confirm or refute this interpretation more directly.

Bilirubin has well-recognized antioxidant and anti-inflammatory activities, with the observed increased plaque destabilization in bilirubin-deficient *Bvra*$^{-/-}$*Apoe*$^{-/-}$ TS mice likely explained by an increase in inflammation and associated pro-oxidant activities. Thus, the present histological, biochemical, proteomics, and in vivo imaging studies reveal unstable plaque of *Bvra*$^{-/-}$*Apoe*$^{-/-}$ TS mice to have increased infiltration, activation, and degranulation of leukocytes and especially neutrophils and this to be associated with increased extracellular matrix degradation and activity of the pro-oxidant enzyme MPO. MPO-derived hypochlorous acid is well known to activate metalloproteinases[36] and directly degrade collagen,[37] a major constituent of the fibrous cap, thereby providing a clear rationale of the mechanism by which cap thinning is enhanced in *Bvra*$^{-/-}$*Apoe*$^{-/-}$ compared with *Bvra*$^{+/+}$*Apoe*$^{-/-}$ TS mice (Figure 3). This interpretation is consistent with the observation that MPO destabilizes plaque in the *Apoe*$^{-/-}$ TS mouse model,[14] as well as humans studies reporting a positive association between circulating bilirubin concentrations and the fibrous content in culprit plaque, as assessed using intravascular ultrasound.[24] At a molecular level, bilirubin does not inhibit MPO activity directly but effectively scavenges the major product of MPO activity, that is, hypochlorous acid.[38] In doing so, bilirubin protects target proteins from hypochlorous acid–mediated oxidation,[38] consistent with the observed decrease in chlorotyrosine in unstable plaque of *Bvra*$^{-/-}$*Apoe*$^{-/-}$ compared with *Bvra*$^{+/+}$*Apoe*$^{-/-}$ TS mice (Figure 7E). We suggest that in the case of unstable human coronary plaque,

Downloaded from http://ahajournals.org by on July 10, 2023

the concentrations of bilirubin are increased as a compensatory process to counter harmful effects of MPO-derived oxidants on the constituents of the fibrous cap, therefore, showing a positive association between bilirubin and MPO activity. Whereas, in *Bvra*$^{-/-}$*Apoe*$^{-/-}$ TS mice, the absence of antioxidant protection by bilirubin to counteract MPO-derived oxidants lead to a further destabilization of unstable plaque (Figure 3).

The almost complete absence of bilirubin from plasma makes *Bvra*$^{-/-}$ mice a useful tool to address the physiological roles of bilirubin,[12] although this approach does not allow to directly demonstrate the putative protective activities of the bile pigment. In this context, the recently developed mouse model with humanized *UGT1A1*28* is of potential interest. Unlike global *Ugt1a1*$^{-/-}$ mice, ≈90% of the newborn animals survive to adulthood and adult *UGT1A1*28* mice have bilirubin plasma concentrations of ≈35 µM.[10,11] Therefore, future studies applying the TS model to crosses of humanized *Ugta1a* with *Apoe*$^{-/-}$ mice are warranted. Also, bilirubin nanoparticles have been reported as a novel tool to increase bilirubin concentrations in vivo[39] and thus may be suitable to test the effect of exogenous bilirubin on plaque stability in the *Apoe*$^{-/-}$ TS mouse model.

In conclusion, our data show that bilirubin deficiency in response to global deletion of *Bvra* generate a proatherogenic phenotype in *Apoe*$^{-/-}$ mice including increased plaque inflammation and oxidative stress that selectively enhances destabilization of unstable plaque, consistent with a causal relationship between circulating bilirubin concentrations and CVD outcome. Our studies support the notion that modest increases in circulating bilirubin may be worthy to consider as a strategy to lower the risk of CVD.

ARTICLE INFORMATION

Received December 12, 2022; revision received February 23, 2023; accepted February 27, 2023.

Affiliations

Heart Research Institute (W.C., S.T., C.P.S., S.M.Y.K., J.N., N.L.V., X.S.W., R.S.), School of Life and Environmental Sciences (R.S.), and Faculty of Medicine and Health (W.C., S.T., C.P.S., X.S.W.), The University of Sydney, Australia. St. Vincent's Hospital, Sydney, Australia (J.N.). University of New South Wales, Sydney, Australia (J.N.). Victor Chang Cardiac Research Institute, Sydney, Australia (D.N., L.L.D.).

Acknowledgments

We acknowledge the support of Dr Cacang Suarna (Heart Research Institute) with biochemical analyses and Dr David Cheng (Victor Chang Cardiac Research Institute) with histology. We acknowledge the facilities and scientific and technical assistance of Biology Facility, Heart Research Institute, and Biological Resource Imaging Laboratory, University of New South Wales.

Sources of Funding

This work was supported by the National Health and Medical Research Council of Australia (NHMRC) program grant APP1052616 to R. Stocker. R. Stocker also acknowledges support from an NHMRC Senior Principal Research Fellowship APP1111632 and an NSW Health Senior Scientist grant. J. Nadel is supported by scholarships from the NHMRC, the National Heart Foundation of Australia, and the University of New South Wales (UNSW). W. Chen was supported by scholarships from UNSW and the China Scholarship Council.

Disclosures

None.

Supplemental Material

Supplemental Materials and Methods
References 40–51
Tables S1–S3
Figures S1–S8

REFERENCES

1. Anderson JL, Morrow DA. Acute myocardial infarction. *N Engl J Med*. 2017;376:2053–2064. doi: 10.1056/NEJMra1606915
2. Kunutsor SK, Bakker SJ, Gansevoort RT, Chowdhury R, Dullaart RP. Circulating total bilirubin and risk of incident cardiovascular disease in the general population. *Arterioscler Thromb Vasc Biol*. 2015;35:716–724. doi: 10.1161/ATVBAHA.114.304929
3. Lin JP, O'Donnell CJ, Schwaiger JP, Cupples LA, Lingenhel A, Hunt SC, Yang S, Kronenberg F. Association between the UGT1A1*28 allele, bilirubin levels, and coronary heart disease in the Framingham Heart Study. *Circulation*. 2006;114:1476–1481. doi: 10.1161/CIRCULATIONAHA.106.633206
4. Stocker R, Yamamoto Y, McDonagh AF, Glazer AN, Ames BN. Bilirubin is an antioxidant of possible physiological importance. *Science*. 1987;235:1043–1046. doi: 10.1126/science.3029864
5. Neuzil J, Stocker R. Free and albumin-bound bilirubin is an efficient co-antioxidant for a-tocopherol, inhibiting plasma and low density lipoprotein lipid peroxidation. *J Biol Chem*. 1994;269:16712–16719.
6. Dong H, Huang H, Yun X, Kim DS, Yue Y, Wu H, Sutter A, Chavin KD, Otterbein LE, Adams DB, et al. Bilirubin increases insulin sensitivity in leptin-receptor deficient and diet-induced obese mice through suppression of ER stress and chronic inflammation. *Endocrinology*. 2014;155:818–828. doi: 10.1210/en.2013-1667
7. Wang WW, Smith DL, Zucker SD. Bilirubin inhibits iNOS expression and NO production in response to endotoxin in rats. *Hepatology*. 2004;40:424–433. doi: 10.1002/hep.20334
8. Vogel ME, Idelman G, Konaniah ES, Zucker SD. Bilirubin prevents atherosclerotic lesion formation in low-density lipoprotein receptor-deficient mice by inhibiting endothelial VCAM-1 and ICAM-1 signaling. *J Am Heart Assoc*. 2017;6:e004820. doi: 10.1161/JAHA.116.004820
9. Chen W, Tumanov S, Fazakerley D, Cantley J, James DE, Dunn LL, Shaik T, Suarna C, Stocker R. Bilirubin deficiency renders mice susceptible to hepatic steatosis in the absence of insulin resistance. *Redox Biol*. 2021;47:102152. doi: 10.1016/j.redox.2021.102152
10. Hinds TD Jr, Hosick PA, Chen S, Tukey RH, Hankins MW, Nestor-Kalinoski A, Stec DE. Mice with hyperbilirubinemia due to Gilbert's syndrome polymorphism are resistant to hepatic steatosis by decreased serine 73 phosphorylation of PPARα. *Am J Physiol Endocrinol Metab*. 2017;312:E244–E252. doi: 10.1152/ajpendo.00396.2016
11. Fujiwara R, Nguyen N, Chen S, Tukey RH. Developmental hyperbilirubinemia and CNS toxicity in mice humanized with the UDP glucuronosyltransferase 1 (UGT1) locus. *Proc Natl Acad Sci USA*. 2010;107:5024–5029. doi: 10.1073/pnas.0913290107
12. Chen W, Maghzal GJ, Ayer A, Suarna C, Dunn LL, Stocker R. Absence of the biliverdin reductase-a gene is associated with increased endogenous oxidative stress. *Free Radic Biol Med*. 2018;115:156–165. doi: 10.1016/j.freeradbiomed.2017.11.020
13. Chen YC, Bui AV, Diesch J, Manasseh R, Hausding C, Rivera J, Haviv I, Agrotis A, Htun NM, Jowett J, et al. A novel mouse model of atherosclerotic plaque instability for drug testing and mechanistic/therapeutic discoveries using gene and microRNA expression profiling. *Circ Res*. 2013;113:252–265. doi: 10.1161/CIRCRESAHA.113.301562
14. Rashid I, Maghzal GJ, Chen YC, Cheng D, Talib J, Newington D, Ren M, Vajandar SK, Searle A, Maluenda A, et al. Myeloperoxidase is a potential molecular imaging and therapeutic target for the identification and stabilization of high-risk atherosclerotic plaque. *Eur Heart J*. 2018;39:3301–3310. doi: 10.1093/eurheartj/ehy419
15. Bowry VW, Stanley KK, Stocker R. High density lipoprotein is the major carrier of lipid hydroperoxides in fasted human plasma. *Proc Natl Acad Sci USA*. 1992;89:10316–10320. doi: 10.1073/pnas.89.21.10316
16. Stocker R, Keaney JF Jr. Role of oxidative modifications in atherosclerosis. *Physiol Rev*. 2004;84:1381–1478. doi: 10.1152/physrev.00047.2003
17. Bayer SB, Maghzal G, Stocker R, Hampton MB, Winterbourn CC. Neutrophil-mediated oxidation of erythrocyte peroxiredoxin 2 as a potential marker

Downloaded from http://ahajournals.org by on July 10, 2023

of oxidative stress in inflammation. *FASEB J.* 2013;27:3315–3322. doi: 10.1096/fj.13-227298
18. Letters JM, Witting PK, Christison JK, Westin Eriksson A, Pettersson K, Stocker R. Time-dependent changes to lipids and antioxidants in plasma and aortas of apolipoprotein E knockout mice. *J Lipid Res.* 1999;40:1104–1112.
19. Cheng D, Talib J, Stanley CP, Rashid I, Michaëlsson E, Lindstedt EL, Croft KD, Kettle AJ, Maghzal G, Stocker R. Inhibition of myeloperoxidase attenuates endothelial dysfunction in mouse models of vascular inflammation and atherosclerosis. *Arterioscl Thromb Vasc Biol.* 2019;39:1448–1457. doi: 10.1161/ATVBAHA.119.312725
20. Fricker ZP, Pedley A, Massaro JM, Vasan RS, Hoffmann U, Benjamin EJ, Long M. Liver fat is associated with markers of inflammation and oxidative stress in analysis of data from the Framingham Heart Study. *Clin Gastroenterol Hepatol.* 2019;17:1157–1164.e4. doi: 10.1016/j.cgh.2018.11.037
21. O'Sullivan JF, Morningstar JE, Yang Q, Zheng B, Gao Y, Jeanfavre S, Scott J, Fernandez C, Zheng H, O'Connor S, et al. Dimethylguanidino valeric acid is a marker of liver fat and predicts diabetes. *J Clin Invest.* 2017;127:4394–4402. doi: 10.1172/JCI95995
22. Kawamura K, Ishikawa K, Wada Y, Kimura S, Matsumoto H, Kohro T, Itabe H, Kodama T, Maruyama Y. Bilirubin from heme oxygenase-1 attenuates vascular endothelial activation and dysfunction. *Arterioscler Thromb Vasc Biol.* 2005;25:155–160. doi: 10.1161/01.ATV.0000148405.18071.6a
23. Daugherty A, Tall AR, Daemen MJAP, Falk E, Fisher EA, García-Cardeña G, Lusis AJ, Owens A 3rd, Rosenfeld ME, Virmani R. Recommendation on design, execution, and reporting of animal atherosclerosis studies: a scientific statement from the American Heart Association. *Circ Res.* 2017;121:e53–e79. doi: 10.1161/RES.0000000000000169
24. Zhu KF, Wang YM, Wang YQ, Wang NF. The relationship between serum levels of total bilirubin and coronary plaque vulnerability. *Coron Artery Dis.* 2016;27:52–58. doi: 10.1097/MCA.0000000000000309
25. Raffel OC, Merchant FM, Tearney GJ, Chia S, Gauthier DD, Pomerantsev E, Mizuno K, Bouma BE, Jang IK. In vivo association between positive coronary artery remodelling and coronary plaque characteristics assessed by intravascular optical coherence tomography. *Eur Heart J.* 2008;29:1721–1728. doi: 10.1093/eurheartj/ehn286
26. Narula J, Nakano M, Virmani R, Kolodgie FD, Petersen R, Newcomb R, Malik S, Fuster V, Finn AV. Histopathologic characteristics of atherosclerotic coronary disease and implications of the findings for the invasive and noninvasive detection of vulnerable plaques. *J Am Coll Cardiol.* 2013;61:1041–1051. doi: 10.1016/j.jacc.2012.10.054
27. Kopriva D, Kisheev A, Meena D, Pelle S, Karnitsky M, Lavoie A, Buttigieg J. The nature of iron deposits differs between symptomatic and asymptomatic carotid atherosclerotic plaques. *PLoS One.* 2015;10:e0143138. doi: 10.1371/journal.pone.0143138
28. Michel JB, Virmani R, Arbustini E, Pasterkamp G. Intraplaque haemorrhages as the trigger of plaque vulnerability. *Eur Heart J.* 2011;32:1977–1985, 1985a, 1985b, 1985c. doi: 10.1093/eurheartj/ehr054
29. Cheng C, Noordeloos AM, Jeney V, Soares MP, Moll F, Pasterkamp G, Serruys PW, Duckers HJ. Heme oxygenase 1 determines atherosclerotic lesion progression into a vulnerable plaque. *Circulation.* 2009;119:3017–3027. doi: 10.1161/CIRCULATIONAHA.108.808618
30. Ayer A, Zarjou A, Agarwal A, Stocker R. Heme oxygenases in cardiovascular health and disease. *Physiol Rev.* 2016;96:1449–1508. doi: 10.1152/physrev.00003.2016
31. Nadel J, Tumanov S, Kong SMY, Chen W, Giannotti N, Sivasubramanian V, Rashid I, Ugander M, Jabbour A, Stocker R. Intraplaque myeloperoxidase activity as biomarker of unstable atheroma and adverse clinical outcomes in human atherosclerosis. *JACC Adv.* 2022. In press.
32. Hazen SL, Heinecke JW. 3-chlorotyrosine, a specific marker of myeloperoxidase-catalyzed oxidation, is markedly elevated in low density lipoprotein isolated from human atherosclerotic intima. *J Clin Invest.* 1997;99:2075–2081. doi: 10.1172/JCI119379
33. Duell PB, Welty FK, Miller M, Chait A, Hammond G, Ahmad Z, Cohen DE, Horton JD, Pressman GS, Toth PP; American Heart Association Council on Arteriosclerosis, Thrombosis and Vascular Biology; Council on Hypertension; Council on the Kidney in Cardiovascular Disease; Council on Lifestyle and Cardiometabolic Health; and Council on Peripheral Vascular Disease. Nonalcoholic fatty liver disease and cardiovascular risk: a scientific statement from the American Heart Association. *Arterioscler Thromb Vasc Biol.* 2022;42:e168–e185. doi: 10.1161/ATV.0000000000000153
34. Wen G, Yao L, Hao Y, Wang J, Liu J. Bilirubin ameliorates murine atherosclerosis through inhibiting cholesterol synthesis and reshaping the immune system. *J Transl Med.* 2022;20:1. doi: 10.1186/s12967-021-03207-4
35. Davies MJ, Thomas A. Thrombosis and acute coronary-artery lesions in sudden cardiac ischemic death. *N Engl J Med.* 1984;310:1137–1140. doi: 10.1056/NEJM198405033101801
36. Fu X, Kassim SY, Parks WC, Heinecke JW. Hypochlorous acid oxygenates the cysteine switch domain of pro-matrilysin (MMP-7). A mechanism for matrix metalloproteinase activation and atherosclerotic plaque rupture by myeloperoxidase. *J Biol Chem.* 2001;276:41279–41287. doi: 10.1074/jbc.M106958200
37. Hawkins CL, Davies MJ. Role of myeloperoxidase and oxidant formation in the extracellular environment in inflammation-induced tissue damage. *Free Radic Biol Med.* 2021;172:633–651. doi: 10.1016/j.freeradbiomed.2021.07.007
38. Stocker R, Peterhans E. Antioxidant properties of conjugated bilirubin and biliverdin: biologically relevant scavenging of hypochlorous acid. *Free Radic Res Comms.* 1989;6:57–66. doi: 10.3109/10715768909073428
39. Lee Y, Kim H, Kang S, Lee J, Park J, Jon S. Bilirubin nanoparticles as a nanomedicine for anti-inflammation therapy. *Angew Chem Int Ed Engl.* 2016;55:7460–7463. doi: 10.1002/anie.201602525
40. Stary HC, Chandler AB, Dinsmore RE, Fuster V, Glagov S, Insull WJ, Rosenfeld ME, Schwartz CJ, Wagner WD, Wissler RW. A definition of advanced types of atherosclerotic lesions and a histological classification of atherosclerosis. A report from the Committee on Vascular Lesions of the Council on Arteriosclerosis, American Heart Association. *Arterioscler Thromb Vasc Biol.* 1995;15:1512–1531. doi: 10.1161/01.atv.15.9.1512
41. Stary HC. Natural history and histological classification of atherosclerotic lesions: an update. *Arterioscler Thromb Vasc Biol.* 2000;20:1177–1178. doi: 10.1161/01.atv.20.5.1177
42. Sattler W, Mohr D, Stocker R. Rapid isolation of lipoproteins and assessment of their peroxidation by HPLC postcolumn chemiluminescence. *Methods Enzymol.* 1994;233:469–489. doi: 10.1016/s0076-6879(94)33053-0
43. Yamamoto Y, Brodsky MH, Baker JC, Ames BN. Detection and characterization of lipid hydroperoxides at picomole levels by high-performance liquid chromatography. *Anal Biochem.* 1987;160:7–13. doi: 10.1016/0003-2697(87)90606-3
44. Behrens WA, Madere R. A highly sensitive high-performance liquid chromatography method for the estimation of ascorbic and dehydroascorbic acid in tissues, biological fluids, and foods. *Anal Biochem.* 1987;165:102–107. doi: 10.1016/0003-2697(87)90206-5
45. Frei B, Kim M, Ames BN. Ubiquinol-10 is an effective lipid-soluble antioxidant at physiological concentrations. *Proc Natl Acad Sci USA.* 1990;87:4879–4883. doi: 10.1073/pnas.87.12.4879
46. Talib J, Maghzal GJ, Cheng D, Stocker R. Detailed protocol to assess *in vivo* and *ex vivo* myeloperoxidase activity in mouse models of vascular inflammation and disease using hydroethidine. *Free Radic Biol Med.* 2016;97:124–135. doi: 10.1016/j.freeradbiomed.2016.05.004
47. Vigder N, Suarna C, Corcilius L, Nadel J, Chen W, Payne RJ, Tumanov S, Stocker R. An improved method for the detection of myeloperoxidase chlorinating activity in biological systems using the redox probe hydroethidine. *Free Radic Biol Med.* 2023;195:23–35. doi: 10.1016/j.freeradbiomed.2022.12.014
48. Martinic G, Hazell L, Stocker R. Vascular microdissection, perfusion, and excision of the murine arterial tree for use in atherogenic disease investigations. *Contemp Top Lab Anim Sci.* 2003;42:47–53.
49. Sluimer JC, Gijbels MJ, Heeneman S. Detection of intraplaque hemorrhage in mouse atherosclerotic lesions. *Methods Mol Biol.* 2015;1339:339–348. doi: 10.1007/978-1-4939-2929-0_24
50. Talib J, Hains PG, Tumanov S, Hodson M, Robinson PJ, Stocker R. A barocycler-based concurrent multi-omics method to assess molecular changes associated with atherosclerosis using small amounts of arterial tissue from a single mouse. *Anal Chem.* 2019;91:12670–12679. doi: 10.1021/acs.analchem.9b01842
51. Okuda S, Watanabe Y, Moriya Y, Kawano S, Yamamoto T, Matsumoto M, Takami T, Kobayashi D, Araki N, Yoshizawa AC, et al. jPOSTrepo: an international standard data repository for proteomes. *Nucleic Acids Res.* 2017;45:D1107–D1111. doi: 10.1093/nar/gkw1080

Downloaded from http://ahajournals.org by on July 10, 2023